Transition kinetics of self-assembled supramolecular dodecagonal quasicrystal and Frank-Kasper σ phases in AB_n dendron-like giant molecules

Xueyan Feng,[1] Gengxin Liu,[4] Dong Guo,[1] Kening Lang,[1] Ruimeng Zhang,[1] Jiahao Huang,[1] Zebin Su,[1] Yiwen Li,[2] Mingjun Huang,[3] Tao Li[5,6] and Stephen Z. D. Cheng[1,3]**

1. Department of Polymer Science, College of Polymer Science and Polymer Engineering, The University of Akron, Akron, Ohio 44325-3909, U.S.A.
2. College of Polymer Science and Engineering, State Key Laboratory of Polymer Materials Engineering, Sichuan University, Chengdu 610065, China
3. South China Advanced Institute for Soft Matter Science and Technology, South China University of Technology, Guangzhou 510640, China
4. Center for Advanced Low-dimension Materials, Donghua University, Shanghai 201620, China
5. Department of Chemistry and Biochemistry, Northern Illinois University, DeKalb, Illinois 60115, United States
6. X-ray Science Division, Advanced Photon Source, Argonne National Laboratory, Argonne, Illinois, 60439, U.S.A.

E-mail: scheng@uakron.edu (S. Z. D. C.), taoli@aps.anl.gov (T. L.)

TOC Graphic

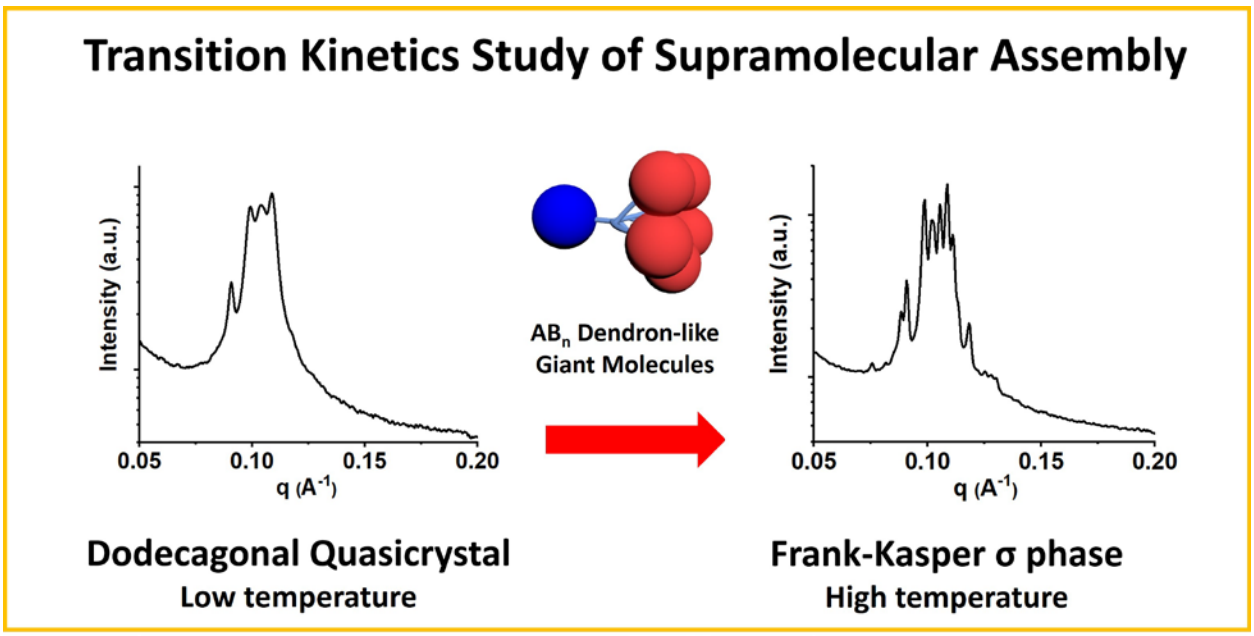
Transition Kinetics Study of Supramolecular Assembly
Intensity (a.u.)
0.05
0.10
0.15
0.20
q (A-1)
ABn Dendron-like
Giant Molecules
Intensity (a.u.)
0.05
0.10
0.15
0.20
q (A-1)
Dodecagonal Quasicrystal
Low temperature
Frank-Kasper σ phase
High temperature

Abstract:

A series of non-crystalline AB_n dendron-like giant molecules DPOSS-$MPOSS_n$ (n = 2-6, DPOSS: hydrophilic polyhedral oligomeric silsesquioxane (POSS) cage; MPOSS: hydrophobic POSS cage) were synthesized. These samples present a thermodynamically stable phase formation sequence from hexagonal cylinder phase (plane group of *P6mm*), to Frank-Kasper (F-K) A15 phase (space group of $Pm\bar{3}n$), and further to F-K σ phase (space group of $P4_2/mnm$), with increasing the number of MPOSS in single molecule (n, from 2 to 6). Moreover, for DPOSS-$MPOSS_5$ and DPOSS-$MPOSS_6$, an intriguing dodecagonal quasicrystal (DQC) structure has been identified and revealed as a kinetic favorable metastable phase at lower temperatures, while the thermodynamically stable phase is σ phase. The detailed investigation of the transition kinetics between the DQC and σ phase in these samples makes it be possible to identify how the self-assembly directs the phase transition in terms of molecular and supramolecular aspects.

Recently, spherically packed Frank-Kasper (F-K) phases[1,2] as well as dodecagonal quasicrystal (DQC) phase[3,4] have been frequently reported in addition to the conventional phase structures such as lamellar (LAM), double gyroids (DG), hexagonal packed cylinder (HEX) and body-centered-cubic (BCC) phases in different types of soft material systems such as dendrimers,[4-11] block copolymers,[12-19] colloidal particles,[20] and giant molecules[21-26] etc. To form F-K and DQC phases, their geometry, topology and function of molecules play important roles. Molecules usually assemble into spherical motifs first, and then these motifs are further organized into those complex spherical phases. In the past two decades, many studies have demonstrated temperature dependences on the supramolecular lattice formation. For example, in the dendron systems, transition master sequences from columnar phase, to F-K A15, to F-K σ and further to BCC phase, as well as transition sequence of DQC to F-K σ phase, and further to isotropic state have been observed upon heating.[4,27] In diblock copolymer systems, different supramolecular phases such as F-K σ, DQC, BCC, F-K C14 and F-K C15 phases have been identified under different and specific thermal annealing conditions; the stability relationship among DQC, F-K σ and BCC phases has been studied that for a single component diblock copolymer (poly(isoprene-b-lactide)): BCC phase is demonstrated as the stable phase at higher temperature range and σ phase is stable at lower temperature range while DQC phase also occurs as a metastable phase at the lowest temperature range [13-15,28].

The question remained is how to recognize their thermodynamic formation/transition pathways and how fast these structure formations will be: a classical kinetic issue in these self-assembled phase behaviors. Note that these individual motifs involved are much larger than those crystalline units we usually deal with, such as atoms and molecules in small molecules or parts of molecules in macromolecules.

In our previous studies, we have prepared a set of AB_n dendron-like giant molecules constructed by linking one hydrophilic polyhedral oligomeric silsesquioxane (POSS) cage (functionalized with fourteen hydroxyl groups, DPOSS) with different numbers of hydrophobic POSS cages (functionalized with seven isobutyl groups, BPOSS).[23] Diverse phase formation behaviors including F-K A15 and σ phase could be observed. However, BPOSS in these materials tend to crystallize, which narrows temperature window for studying the supramolecular crystal structures and disturbs the investigation of kinetic pathways and formation mechanisms of these F-K phases.

We thus prepared a series of AB_n dendron-like giant molecules including non-crystalline hydrophobic POSS cages (which is functionalized with seven relative long branched alkyl chains, MPOSS). This prohibits crystallization in the molecular level. Potential phase transitions would take place only in the supramolecular level. These molecules possess precise chemical structure with uniform molecular masses. Their molecular shapes and chemical structures are shown in Figures S1 and S2 (supporting information (SI)). The detailed synthetic route and chemical characterizations (^{1}H-nuclrar magnetic resonance (NMR), ^{13}C-NMR and Matrix-assisted Laser Desorption/Ionization Time-of-Flight (MALDI-TOF) mass spectra) are described in SI (Figures S3-S6). These molecules have a large temperature window between glass transition temperature and disorder temperature (room temperature to ~160 °C, DSC data in Figure S7) as well as suitable kinetics time window (~10^3 sec.), which facilitate the investigation of the potential phase transitions.

As shown in Figure 1, these molecules exhibit rich self-assemble behaviors. Both DPOSS-$MPOSS_2$ and DPOSS-$MPOSS_3$ form hexagonal packed cylinders phase (Figures 1a and 1b), while DPOSS-$MPOSS_4$ forms F-K A15 phase (Figure 1c). In-situ SAXS experiments at different

temperatures indicate that HEX and A15 phases are the only ordered phases can be observed up to their disorder temperatures (Figures S8-S10, detailed analysis of phase identifications of DPOSS-MPOSS$_2$, DPOSS-MPOSS$_3$ and DPOSS-MPOSS$_4$ see SI Section 3). The reason for these phase formation is due to changing molecular geometry from "fan-like" shape to "cone-like" shape, [23,29] similar with the reported results in crystalline AB$_n$ dendron-like molecules.

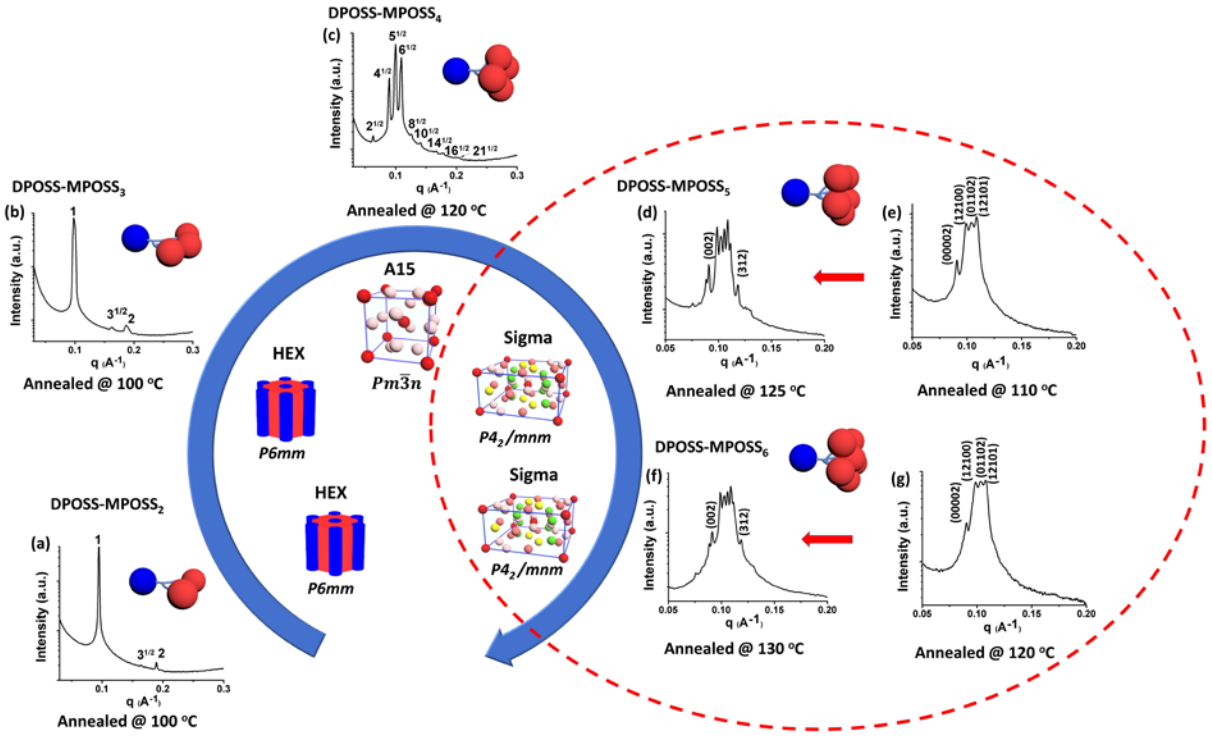

Figure 1. Phase diagram and corresponding SAXS characterization of the series of AB$_n$ non-crystalline dendron-like giant molecules. (a) DPOSS-MPOSS$_2$ and (b) DPOSS-MPOSS$_3$ both form HEX structures; (c) DPOSS-MPOSS$_4$ forms F-K A15 structure; (d) DPOSS-MPOSS$_5$ after annealed at 110 °C forms DQC structure; (e) DPOSS-MPOSS$_5$ after annealed at 125 °C forms F-K σ structure; (f) DPOSS-MPOSS$_6$ after annealed at 120 °C forms DQC structure; and (g) DPOSS-MPOSS$_6$ after annealed at 130 °C forms F-K σ structure. All the samples were annealed for 20 hours at targeted temperatures and characterized at room temperature.

For DPOSS-MPOSS$_5$, two distinct SAXS patterns can be identified after the samples are quenched from disordered state and then, isothermally kept at 110 °C and 125 °C, respectively (Figures 1d and 1e). At 110 °C, SAXS pattern exhibits four strong diffractions (Figure 1d), which can be assigned to be DQC phase, with these four diffractions indexed as (00002), (12100), (01102), and (12101), respectively, in a 5D coordination.[14] However, at 125 °C, a completely different SAXS pattern with more than a dozen of diffractions was found (Figure 1e). This pattern can be clearly identified and indexed to be F-K σ phase (diffraction peak assignments in Table S2). In-situ temperature-resolved SAXS experiments to observe these two phases are also shown in Figure S11. We can thus observe two phase structures in this DPOSS-MPOSS$_5$: the DQC phase at lower temperatures and the F-K σ phase at higher temperatures.

Similarly, DPOSS-MPOSS$_6$, which has six hydrophobic MPOSS cages, shows DQC phase (isothermally kept at 120 °C) and σ phase (isothermally kept at 130 °C) (Figures 1f and 1g) again. The σ pattern assignments are shown in Table S3.

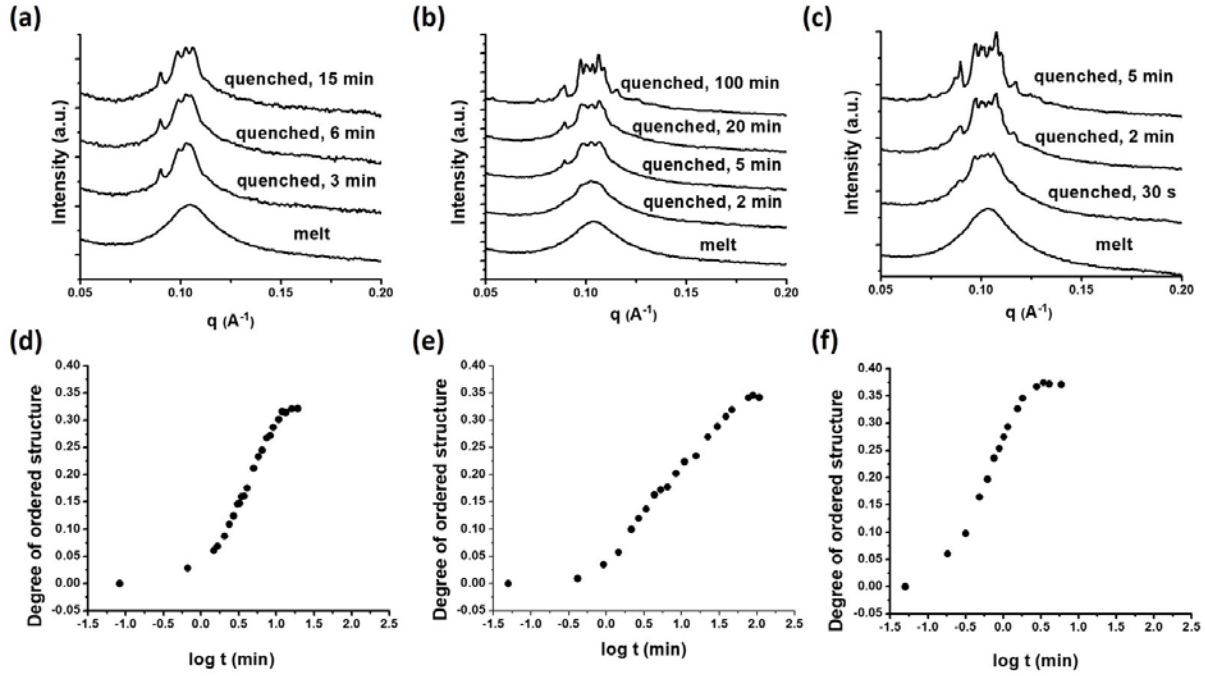

Figure 2. SAXS results for ordering kinetics of DPOSS-MPOSS$_5$. (a-c) in-situ characterized SAXS results with different isothermal time, the samples were disordered at 150 °C and then quenched to different isothermal temperatures (with a rate of 100 °C/min): (a) 110 °C, (b) 118 °C, (c) 125 °C (the SAXS results of these samples for more isothermal time points can be seen in Figures S12, S14 and S16); (d-f) relationship of degree of structural order of sample versus isothermal time, based on isothermal in-situ SAXS results in Figure S12, S14 and S16: disordered sample was quenched to different isothermal temperatures (d) 110 °C, (e) 118 °C, and (f) 125 °C (the degree of structural order is calculated as $S_{diffraction}/S_{pattern}$, $S_{diffraction}$ is the integrated area of all the feature diffraction peaks, $S_{pattern}$ is the integrated area of the corresponding SAXS pattern).

We focused investigation on the phase transition behavior of DPOSS-MPOSS$_5$ as an example to study the phase transition kinetics between DQC and F-K σ phases. After sample was quenched from disordered state at 150 °C (where SAXS pattern of sample only shows an amorphous scattering halo) to 110 °C and isothermally kept there, in-situ time-resolved SAXS patterns at different isothermal time are recorded as shown in Figure 2a (also, Figure S12). The degree of structural order of this sample versus isothermal time is plotted in Figure 2d. The degree of structural order reaches to a constant value of about 32% in around 10 minutes. And the corresponding Avrami treatment plot reveals a slope of 1.28, which supposedly represents the average growth dimensionality (n) of ordered structures (Figure S13a). The relatively low n value from Figure S13a is due frequently to the reasons of a decrease of active nuclei and reduction of crystal growth rate with increasing isothermal time.[30]

In the case of quenching DPOSS-MPOSS$_5$ to a higher temperature (125 °C) and isothermally being kept there, the in-situ time-resolved SAXS patterns are shown in Figure 2c (also, Figure S14). The F-K σ phase pattern gradually grows up from disordered halo with increasing isothermal time. The relationships between degree of structural order with isothermal time is shown in Figure 2f. The degree of structural order reaches a constant at around 3 mins with a value about 37%

(Figure 2f); and corresponding Avrami plot is shown in Figure S13b with a slop value (n) of 1.15. In this high-temperature formation process, no trace of DQC phase structure was detected, though we cannot rule out the possibility of effects from DQC phase formation in the very early short time window ($t < 30$ s) due to the short time window and limited SAXS resolution. This phenomenon is so-called "phase stability inversion due to the crystal size".[31] After the σ phase was fully developed at 125 °C, we quenched the sample down to 110 °C and isothermally annealed it at this temperature. The F-K σ phase remains unchanged (Figure S15), suggesting that DQC phase is a metastable phase.

Between these two high and low isothermal temperatures, DPOSS-MPOSS$_5$ at disordered state (150 °C) was also quenched to 118 °C. The sample has been found to form DQC phase at first. And with a relatively long isothermal time (~80 mins), the sample completes a transition from DQC phase into F-K σ phase (Figure 2b, also, Figure S16). The corresponding plot of degree of structural order versus isothermal time in Figure 2e shows a short-time plateau at the time around 5 minutes while the SAXS result still shows a DQC pattern at this plateau; the after growth of degree of structural order happens with phase transition from DQC to F-K σ phase. And finally, σ phase growth saturates at about 80 minutes. Corresponding Avrami plot was shown in Figure S13c. Two processes of growth can be observed: within the first time process where DQC grows, the n value is 1.10, comparable with values observed at 110 °C (Figure S13a); in the following phase transition (from the DQC to the σ phase), the n value is much smaller (0.31), This value does not reflect a less dimensional organization as commonly observed in in liquid crystal transitions, annealing processes in polymer crystals and other soft matters.[30] Rather, the overall kinetics of this transformation takes place due to the fact that growing the σ phase is in expense of the DQC phase and thus, leads to this overall growth following a slower pace and a smaller n value.

To analyze how this transition kinetics between the DQC and F-K σ phases takes place, we investigate the relationships between intensities of characteristic diffractions for each structure and isothermal time at 118 °C (Figure 3). Since (00002) diffraction of DQC phase and (002) diffraction of F-K σ phase possess identical q value (both provide structure information along c axis), we chose this overlapped diffraction as well as (01102) diffraction for DQC phase [$(01102)_{DQC}$], and (312) diffraction for σ phase [$(312)_{\sigma}$] as the characteristic diffractions to investigate. After quenching sample from disordered state, the intensity of diffraction corresponding to $(00002)_{DQC}$ (Figure 3a) reaches to a plateau as the first step after about 5 minutes; and then, the intensity grows again and reaches to maxima at about 80 minutes, which is due to the transition from $(00002)_{DQC}$ to $(002)_{\sigma}$ and further growth of $(002)_{\sigma}$. This can be proven by the observations that the intensity of $(01102)_{DQC}$ grows first, reaches a maximum and then decreases with increasing isothermal time (Figure 3b); as well as the intensity of $(312)_{\sigma}$ remains close to baseline in the first 5 minutes and then, grow to maxim at about 80 minutes (Figure 3c). The F-K σ phase thus develops in the expense of DQC phase at least to certain degree. Also, Figure 2e shows degree of structural order of the sample reaches a maximum of ~34% at a prolonged isothermal time, similar to the final degree of structural order of this sample isothermally kept at 110 °C (Figure 2d) and 125 °C (Figure 2f). This observation further supports a solid-solid conversion of DQC phase into F-K σ phase rather than both phases separately develop from disordered state, matching with the conclusion from the kinetic data (Figure S13).

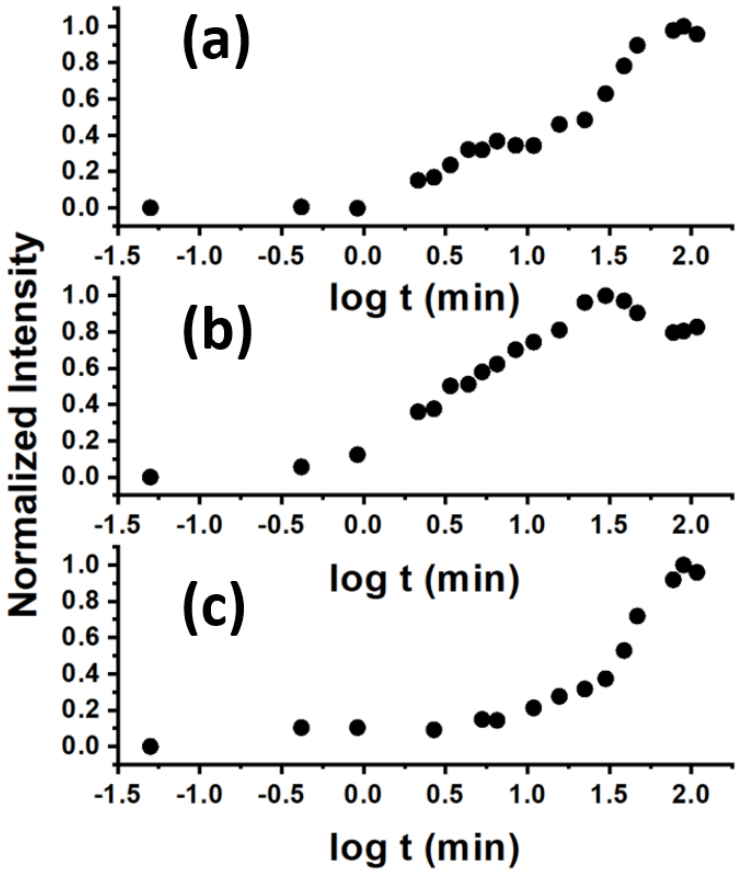

Figure 3. Relationship between intensity of featured SAXS diffraction peaks of DPOSS-MPOSS$_5$ sample and isothermal time. The intensities of peaks are determined by subtracting the intensity of corresponding amorphous halo from the experimental X-ray pattern, and then normalized by the maximum of the peak intensity. The sample was quenched from the disordered melt to 118 °C at 100 °C/min: (a) (00002) peak for the DQC pattern as well as (002) peak for the F-K σ phase pattern, (b) (01102) peak for the DQC pattern, (c) (312) peak for the F-K σ phase pattern.

The phase formation and transition machnisem is further studied with the relationship between a quantity of 10% order structural formation time (log($t_{0.1}$)) and isothermal temperature, as shown in Figure 4.[31,32] In the figure, faster kinetics is represented by less isothermal time needed to reach 10% degree of structural formation. It is found that DQC formation kinetics is slowed down with increasing isothermal temperature (as shown by the red points); while in σ phase formation region, the kinetics becomes faster with increasing isothermal temperature first and then, it slows down

when the isothermal temperature approaches to the disorder temperature (as shown by blue points), namely, a "U" shaped relation can be found for the F-K σ phase formation. When the disordered melt sample was quenched to 90 °C and annealed at this temperature, no ordered structure could be observed with a long annealing time (2 days). The deceleration of phase formation would be due to "ergodicity temperature" (T_{erg}), a critical temperature related with the dramatically change of molecule exchange/mobility[13,14] When the sample is quenched to $T < T_{erg}$, the molecule exchange/mobility slows dramatically, which inhibits formation of F-K or DQC phases that require redistribution of particle sizes. Thus, we also predict that a "U" shaped relation exists in the DQC phase formation between the ergodicity temperature and ~118 °C. The mechanism for both phase transitions can be deduced as a "nucleation controlled" process.[33] Yet the basic unit of these process is the assembled spherical motif rather than individual molecules in small molecular crystallization or part of a molecule in macromolecular crystallization.

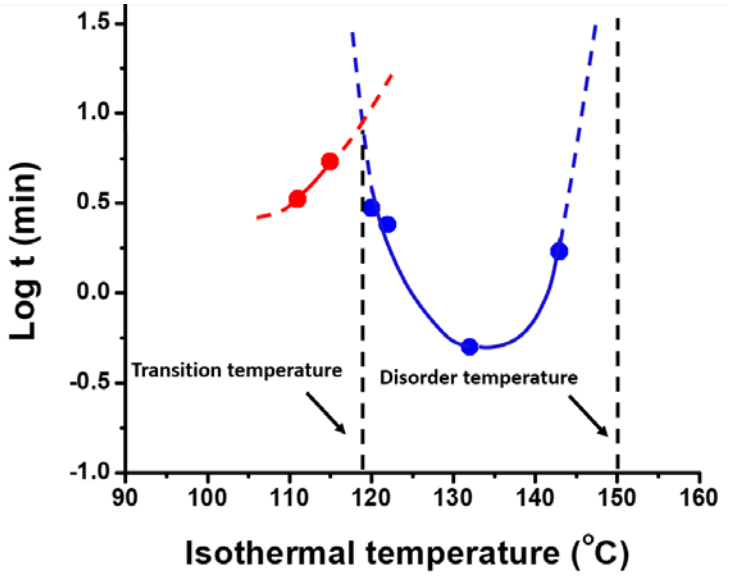

Figure 4. Phase formation mechanism study of DPOSS-MPOSS$_5$. The isothermal annealing time needed for the sample to get to ~10% degree of structural order (Y axis) was recorded for different isothermal temperatures (X axis): red color is for DQC formation, and blue color is for σ phase formation. Estimated trend is also plotted.

Rheological behaviors of materials are also closely related with their supramolecular structures.[13,14,34] Here we investigated the rheological behaviors of DPOSS-MPOSS$_5$ in different ordered state. Figure 5a shows storage *(G')* and loss *(G")* moduli of DPOSS-MPOSS$_5$ sample with increasing temperature at a heating rate of 10 °C/min (oscillatory shear at 10 rad/s). We can observe a plateau of *G'*, which is due to the caging on motifs formed by surrounding molecules. From the disordered state to F-K σ phase, plateau modulus increases from 2×10^5 to 4×10^5 Pa. This increase is attributed to the ordered packing of spherical motifs. During heating, once the sample reaches the disordered state, the *G'* and *G''* come to a terminal crossover.

Black symbols in Figure 5a show *G'* and *G"* of the quenched and disordered sample. They exhibit a trend (from 70 to 90 °C) that may come to terminal crossover at around 100 °C as shown with orange dash line. However, this crossover is interrupted at around 90 °C due to the occurrence of forming DQC phase. This is also illustrated by the SAXS heating experiments as shown in Figure 5b. With increasing temperature of the original quenched and disordered sample, diffraction peaks start to appear. For the sample with DQC phase, its *G'* and *G"* (blue symbols in Figure 5a) show a terminal crossover of *G'* and *G"* at a much higher temperature. From SAXS heating experiment (Figure 5C), DQC structure could not afford to transfer into more ordered σ phase before entering the disordered state at this fast heating rate (10 °C/min). For the sample with F-K σ phase, the crossover temperature for *G'* and *G"* appears to occur at even higher temperature than that of the DQC phase (red symbols). Such extension of elastic plateau to high temperatures is also induced by more stable supramolecular structural packing of σ phase.

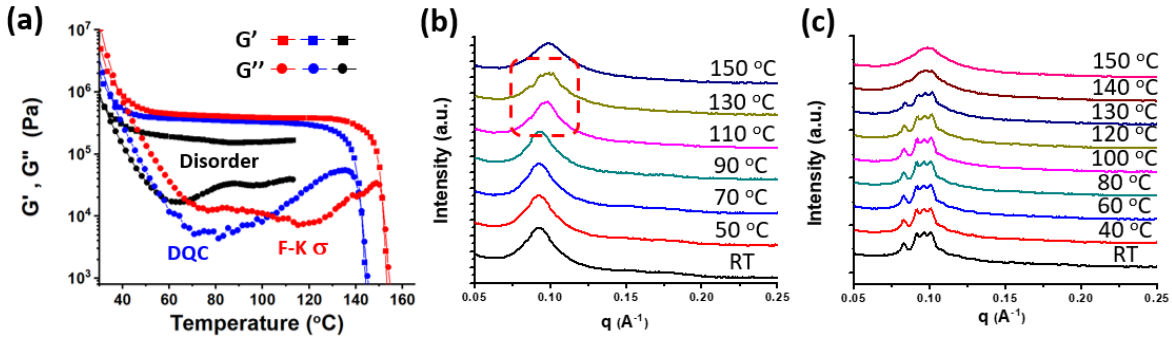

Figure 5. (a) Rheology temperature sweep experiments show the change of *G'* and *G"* shape as in different states of DPOSS-MPOSS$_5$ (the increasing temperature rate is 10 °C/min). The results in different colors are corresponding to different order stages as disordered state (black), DQC phase (blue), F-K σ phase (red), the orange dash line indicates the trend of terminal crossover at around 100 °C for disordered sample. (b) SAXS temperature sweep experiments of DPOSS-MPOSS$_5$ in disordered state (from room temperature to 150 °C, the increasing temperature rate is 10 °C/min), diffraction peaks start to appear when the temperature was increased to 110 °C and 130 °C; (c) SAXS temperature sweep experiments of DPOSS-MPOSS$_5$ in DQC state (from room temperature to 150 °C, the increasing temperature rate is 10 °C/min).

As for DPOSS-MPOSS$_6$, it exhibits identical phase transition from DQC phase to F-K σ phase as indicated by the thermal in-situ SAXS results shown in Figure S17.

Simulation studies indicate that the growth of quasicrystals is controlled by the ability of growing quasicrystal nucleus to incorporate building spherical motifs into the solid phase with minimal rearrangement of these motifs; i.e. during the bulk quasicrystal phase formation, the "growth rule" is the tendency to retain configurations of building motifs rather than copying nucleus surface template to from a traditional crystal. [35] σ phase is a periodic approximant structure to DQC phase. They share similar local tetrahedral closed packing feature. The less ordered DQC could be able to reach a "structural compromise" with the surrounding motifs in a more rapid rate as kinetic favorable phase when the rearrangement ability of the building motifs is limited,

compared with σ phase which requires relative decent rearrangements of the building motifs into crystal lattice.[14] The rearrangement of motifs during phase formation would be a combination of configuration rearrangements of multiple sphere cluster[35] and internal rearrangement of the spheres themselves[14]. However, to better understand the real sub-unit cell information of these complex structures, high fidelity 3D reconstruction studies in the future is necessary. At sufficiently low temperatures, the kinetics of spherical motif's rearrangement to form F-K σ phase would be slow to such a degree that DQC phase formation takes over. Only providing sufficiently long in annealing time or high in temperature, σ phase can grow.

As a summary, for a set of precisely defined non-crystalline DPOSS-MPOSS$_n$ samples, a thermodynamically stable phase sequence from HEX to A15 phase and further to σ phase was reported by increasing the number of MPOSS cages. Specifically, in DPOSS-MPOSS$_5$ and DPOSS-MPOSS$_6$, a transition between DQC phase and F-K σ phase is observed. the phase transition kinetics between DQC and σ phase has been quantitatively investigated with both scattering and rheological experiments. We have found that the DQC phase is a kinetic favorable metastable phase, while F-K σ phase as an ordered approximant of DQC phase is the thermodynamically stable phase. The nucleation-controlled process plays a dominating role in the phase formation of both the DQC and σ phases. This study attempts to explore the structural transition pathways and relationships between different phases, especially the F-K σ phase and DQC phase.

Associated Content

Supporting Information

The supporting information is available free of charge on the ACS Publications website.

Synthetic procedures, characterization methods, detailed calculation and data

Acknowledgment. Acknowledgments: This work was supported by National Science Foundation (DMR-1408872 to S.Z.D.C.) and the Program for Guangdong introducing Innovative and Entrepreneurial Teams (no. 2016ZT06C322). T. Li is thankful for the support from NIU startup. This research used resources of the Advanced Photon Source, a U.S. Department of Energy (DOE) Office of Science User Facility operated for the DOE Office of Science by Argonne National Laboratory under Contract No. DE-AC02-06CH11357.

References

(1) Frank, F. C.; Kasper, J. S. Complex Alloy Structures Regarded as Sphere Packings. I. Definitions and Basic Principles. *Acta Crystallogr.* **1958,** *11*, 184.

(2) Frank, F. C.; Kasper, J. S. Complex Alloy Structures Regarded as Sphere Packings. II. Analysis and Classification of Representative Structures. *Acta Crystallogr.* **1959,** *12*, 483.

(3) Ishimasa, T.; Nissen, H. U.; Fukano, Y. New Ordered State between Crystalline and Amorphous in Ni-Cr Particles. *Phys. Rev. Lett.* **1985,** *55*, 511.

(4) Zeng, X. B.; Ungar, G.; Liu, Y. S.; Percec, V.; Dulcey, A.; Hobbs, J. K. Supramolecular Dendritic Liquid Quasicrystals. *Nature* **2004,** *428*, 157.

(5) Sun, H. J.; Zhang, S. D.; Percec, V. From Structure to Function via Complex Supramolecular Dendrimer Systems. *Chem. Soc. Rev.* **2015,** *44*, 3900.

(6) Rosen, B. M.; Wilson, C. J.; Wilson, D. A.; Peterca, M.; Imam, M. R.; Percec, V. Dendron-mediated Self-assembly, Disassembly, and Self-organization of Complex Systems. *Chem. Rev.* **2009,** *109*, 6275-6540.

(7) Ungar, G.; Liu, Y. S.; Zeng, X. B.; Percec, V.; Cho, W. D. Giant Supramolecular Liquid Crystal Lattice. *Science* **2003,** *299*, 1208.

(8) Ungar, G.; Zeng, X. B. Frank-Kasper, Quasicrystalline and Related Phases in Liquid Crystals. *Soft Matter* **2005,** *1*, 95.

(9) Hudson, S. D.; Jung, H. T.; Percec, V.; Cho, W. D.; Johansson, G.; Ungar, G.; Balagurusamy, V. S. K. Direct Visualization of Individual Cylindrical and Spherical Supramolecular Dendrimers. *Science* **1997,** *278*, 449.

(10) Percec, V.; Cho, W.-D.; Ungar, G.; Yeardley, D. J. P. From Molecular Flat Tapers, Discs, and Cones to Supramolecular Cylinders and Spheres Using Frechet-type Mondendrons Modified on Their Perphery, *Angew. Chem, Int, Ed* **2000,** 39, 1598.

(11) Percec, V.; Cho, W. D.; Moller, M.; Prokhorova, S. A.; Ungar, G.; Yeardley, D. J. P. Design and Structural Analysis of The First Spherical Monodendron Self-organizable in A Cubic Lattice. *J. Am. Chem. Soc.* **2000,** *122*, 4249.

(12) Lee, S.; Bluemle, M. J.; Bates, F. S. Discovery of a Frank-Kasper Sigma Phase in Sphere-Forming Block Copolymer Melts. *Science* **2010,** *330*, 349.

(13) Lee, S.; Leighton, C.; Bates, F. S. Sphericity and Symmetry Breaking in the Formation of Frank-Kasper Phases From One Component Materials. *Proc. Natl. Acad. Sci. U. S. A.* **2014,** *111*, 17723.

(14) Gillard, T. M.; Lee, S.; Bates, F. S. Dodecagonal Quasicrystalline Order in a Diblock Copolymer Melt. *Proc. Natl. Acad. Sci. U. S. A.* **2016,** *113*, 5167.

(15) Kim, K.; Schulze, M. W.; Arora, A.; Lewis, R. M.; Hillmyer, M. A.; Dorfman, K. D.; Bates, F. S. Thermal Processing of Diblock Copolymer Melts Mimics Metallurgy. *Science* **2017,** *356*, 520.

(16) Zhang, J.; Bates, F. S. Dodecagonal Quasicrystalline Morphology in a Poly(styrene-b-isoprene-b-styrene-b-ethylene oxide) Tetrablock Terpolymer. *J. Am. Chem. Soc.* **2012,** *134*, 7636.

(17) Chanpuriya, S.; Kim, K.; Zhang, J.; Lee, S.; Arora, A.; Dorfman, K. D.; Delaney, K. T.; Fredrickson, G. H.; Bates, F. S. Cornucopia of Nanoscale Ordered Phases in Sphere-Forming Tetrablock Terpolymers. *ACS Nano* **2016,** *10*, 4961.

(18) Schulze, M. W.; Lewis, R. M.; Lettow, J. H.; Hickey, R. J.; Gillard, T. M.; Hillmyer, M. A.; Bates, F. S. Conformational Asymmetry and Quasicrystal Approximants in Linear Diblock Copolymers. *Phys. Rev. Lett.* **2017,** *118*.

(19) Reddy, A.; Buckley, M. B.; Arora, A.; Bates, F. S.; Dorfman, K. D.; Grason, G. M. Stable Frank-Kasper Phases of Self-assembled, Soft Matter Spheres. *Proc. Natl. Acad. Sci. U. S. A.* **2018,** *115*, 10233.

(20) Shevchenko, E. V.; Talapin, D. V.; Kotov, N. A.; O'Brien, S.; Murray, C. B. Structural Diversity in Binary Nanoparticle Superlattices. *Nature* **2006,** *439*, 55.

(21) Huang, M. J.; Hsu, C. H.; WANG, J.; Mei, S.; Dong, X. H.; Li, Y. W.; Li, M. X.; Liu, H.; Zhang, W.; Aida, T.; Zhang, W.-B.; Yue, K.; Cheng, S.Z.D. Selective Assemblies of Giant Tetrahedra via Precisely Controlled Positional Interactions. *Science* **2015,** *348*, 424.

(22) Yue, K.; Huang, M.; Marson, R. L.; He, J.; Huang, J.; Zhou, Z.; Wang, J.; Liu, C.; Yan, X.; Wu, K.; Guo, Z.H.; Liu, H.; Zhang, W.; Ni, P.H.; Wesdemiotis, C.; Zhang, W.-B.; Glotzer, S.C.; Cheng, S.Z.D. Geometry Induced Sequence of Nanoscale Frank-Kasper and Quasicrystal Mesophases in Giant Surfactants. *Proc. Natl. Acad. Sci. U. S. A.* **2016,** *113*, 14195.

(23) Feng, X. Y.; Zhang, R. M.; Li, Y. W.; Hong, Y. L.; Guo, D.; Lang, K.; Wu, K. Y.; Huang, M. J.; Mao, J. L.; Wesdemiotis, C.; Nishiyama, Y.; Zhang, W.; Zhang, W.; Miyoshi, T.; Li, T.; Cheng, S.Z.D. Hierarchical Self-Organization of AB(n) Dendron-like Molecules into a Supramolecular Lattice Sequence. *ACS Cent. Sci.* **2017,** *3*, 860.

(24) Zhang, W.; Lu, X. L.; Mao, J. L.; Hsu, C. H.; Mu, G. Y.; Huang, M. J.; Guo, Q. Y.; Liu, H.; Wesdemiotis, C.; Li, T.; Zhang, W.-B.; Li, Y. W.; Cheng, S.Z.D. Sequence-Mandated, Distinct Assembly of Giant Molecules. *Angew. Chem, Int, Ed* **2017,** *56*, 15014.

(25) Lin, Z. W.; Yang, X.; Xu, H.; Sakurai, T.; Matsuda, W.; Seki, S.; Zhou, Y. B.; Sun, J.; Wu, K. Y.; Yan, X. Y.; Zhang, R. M.; Huang, M. J.; Mao, J. L.; Wesdemiotis, C.; Aida, T.; Zhang, W.; Cheng, S.Z.D. Topologically Directed Assemblies of Semiconducting Sphere Rod Conjugates. *J. Am. Chem. Soc.* **2017,** *139*, 18616.

(26) Zhang, W. B.; Yu, X. F.; Wang, C. L.; Sun, H. J.; Hsieh, I. F.; Li, Y. W.; Dong, X. H.; Yue, K.; Van Horn, R.; Cheng, S. Z. D. Molecular Nanoparticles Are Unique Elements for Macromolecular Science: From "Nanoatoms" to Giant Molecules. *Macromolecules* **2014,** *47*, 1221.

(27) Yao, X. H.; Cseh, L.; Zeng, X. B.; Xue, M.; Liu, Y. S.; Ungar, G. R. Body-centred Cubic Packing of Spheres - the Ultimate Thermotropic Assembly Mode for Highly Divergent Dendrons. *Nanoscale Horiz.* **2017,** *2*, 43.

(28) Kim, K.; Arora, A.; Lewis, R. M.; Liu, M. J.; Li, W. H.; Shi, A. C.; Dorfman, K. D.; Bates, F. S. Origins of Low-symmetry Phases in Asymmetric Diblock Copolymer Melts. *Proc. Natl. Acad. Sci. U. S. A.* **2018,** *115*, 847.

(29) Rosen, B. M.; Wilson, D. A.; Wilson, C. J.; Peterca, M.; Won, B.C.; Huang, C. H.; Lipski, L. R; Zeng, X. B.; Ungar, G.; Heiney, P. A.; Percec, V. Predicting the Structure of

Supramolecular Dendrimers Viathe Analysis of Libraries of AB_3 and Constitutional Isomeric AB_2 Biphenylpropyl Ether Self-assembling Dendrons. *J. Am. Chem. Soc.* **2009**, *131*, 17500.

(30) Cheng, S. Z. D.; Wunderlich, B. Modification of the Avrami Treatment of Crystallization to Account for Nucleus and Interface. *Macromolecules* **1988,** *21*, 3327.

(31) Cheng, S. Z. D. Phase Transitions in Polymers: The Role of Metastable States, 1st ed; Elsevier: Oxford, 2008.

(32) Sun, L.; Zhu, L.; Ge, Q.; Quirk, R. P.; Xue, C. C.; Cheng, S. Z. D.; Hsiao, B. S.; Avila-Orta, C. A.; Sics, I.; Cantino, M. E. Comparison of Crystallization Kinetics in Various Nanoconfined Geometries. *Polymer* **2004,** *45*, 2931.

(33) Cheng, S. Z. D.; Lotz, B. Nucleation Control in Polymer Crystallization: Structural and Morphological Probes in Different Length- and Time-scales for Selection Processes. *Philos. Trans. Royal Soc. A* **2003,** *361*, 517.

(34) Liu, G. X.; Feng, X. Y.; Lang, K. N.; Zhang, R. M.; Guo, D.; Yang, S. G.; Cheng, S. Z. D. Dynamics of Shape-Persistent Giant Molecules: Zimm-like Melt, Elastic Plateau, and Cooperative Glass-like. *Macromolecules* **2017,** *50*, 6637.

(35) Keys, A. S.; Glotzer, S. C. How Do Quasicrystals Grow? *Phys. Rev. Lett.* **2007,** *99*.